MULTISCALE DAMAGE ANALYSIS OF LAMINATED COMPOSITE STRUCTURES USING GENERALIZED METHOD OF CELLS THEORY AND ABAQUS

D. Ivančević*, I. Smojver

University of Zagreb, Faculty of Mechanical Engineering and Naval Architecture, Department of Aeronautical Engineering, I. Lučića 5, 10000 Zagreb, Croatia
**divancevic@fsb.hr*

Keywords: multiscale analysis, micromechanical model, failure criteria, Abaqus/Explicit.

Abstract
The High Fidelity Generalized Method of Cells (HFGMC) has been implemented into Abaqus/Explicit in order to model damage processes in composite materials at the micromechanical level. The HFGMC model is implemented into the finite element code Abaqus via user material subroutine VUMAT. The result of the micromechanical procedure is the computation of strain concentration tensors, which relate the strain tensor on the macro-level to the strain tensor of each subcell. This enables calculation of the stress field within the unit cell, based on the constitutive behavior of each subcell. As the stress distribution is determined for the representative unit cells, calculation of failure criteria and constitutive response of the composite are performed on the micro-level. The most frequently used micromechanical failure criteria have been used in this work as well. Parametric analyses using different unit cell shapes and discretization refinement have been performed. Results of micromechanical analyses confirm significant dependence of failure criteria on unit cell type and refinement.

1 Introduction
Failure modes of fiber reinforced materials are closely related to processes within the heterogeneous composite material. In order to get insight into the underlying damage processes of composite materials, a micromechanical model has been coupled to the commercial finite element code Abaqus/Explicit. Coupling between the micromechanical model and the finite element analysis has been achieved using the user material subroutine VUMAT.

The micromechanical model employs an improved version of the High Fidelity Generalized Method of Cells, which has been introduced in [1,2,3]. The HFGMC model belongs to the group of micromechanical models which originated from the Method of Cells (MOC) model, introduced e.g. in [4]. The MOC model discretizes a fiber reinforced material by a representative volume element, or unit cell [4]. The representative cell is in the original model divided into four subcells, of which one represents the fiber while the matrix is represented by the remaining three subcells. An extension of the MOC model is the Generalized Method of Cells (GMC) which allows the composite material unit cell to be represented by an arbitrary number of subcells, enabling modeling of more complex composite materials [5]. In recent publications, the GMC has been used as a micro-model in multiscale analyses, as for example

in [6,7]. The most important drawback of the GMC model is the lack of "normal-shear coupling", which indicates that application of macroscopic normal strains/stresses produces only normal subcell strains/stresses although each subcell might be isotropic, transversely orthotropic or orthotropic. As stated in [3], this deficiency can potentially produce inaccurate results in the presence of cracks, disbonds or porosities. A further drawback of the GMC theory is that the displacement field within the unit cell is linear, making it unsuitable for e.g. wave propagation analyses, as stated in [4].

The lack of normal-shear coupling and the drawbacks caused by the linear displacement field approximation have been later solved by the High Fidelity Generalized Method of Cells as explained in [8]. HFGMC uses a Legendre type polynomial to approximate the displacement field within the subcell, leading to fundamental differences between the HFGMC and GMC, although they share the same concept of unit cell discretization. Comparison of GMC and HFGMC micromechanical analyses can be found for example in [3,9]. The reformulated version of the HFGMC, which has been employed in this work, is in the literature also known as the Finite Volume Direct Averaging Micromechanics (FVDAM), as for example in [3]. The main difference in comparison with the original HFGMC is that it departs from the concept of Generic Cells, significantly reducing the final system of equations by 60% [2,8]. The main drawback of the HFGMC, compared to the preceding micromechanical models (e.g. GMC) is the increased computational time of the HFGMC method. The computational cost of HFGMC is still lower compared to similar FEM analyses, and therefore the HFGMC model presents a good compromise between the accuracy and computational cost.

The methodology used in this work belongs to the group of multiscale analyses, since computations are being performed on two different length scales. More specifically, the solution of the explicit finite element analysis on the macro-level is passed to the micro-level HFGMC analysis, where composite failure criteria are calculated at the constituent level. The micromechanical model has in this work been used to predict composite equivalent properties and predict failure criteria on the micro-level. Damage processes have not been included in the model, since the method is still in the development phase. Consequently, constituent mechanical properties have not been degraded during the current research. The employed multiscale framework has been tested on a very simple finite element model in order to verify the micromechanical analysis and failure criteria.

2 Micromechanical model

2.1 HFGMC model

The HFGMC model discretizes the representative volume element of the heterogeneous material using N_β x $N\gamma$ subcells, which can be either fiber or matrix subcells. In order to study the effect of unit cell arrangement, three types of unit cells have been investigated as shown in Figure 1. The first unit cell incorporates a single fiber at the unit cell centre. The second unit cell discretizes the composite material with four fibers, with fiber centers located at the unit cell corners. The third unit cell is a combination of the first and second unit cells, with fiber centers at unit cell corners and a single fiber located at the unit cell centre. All unit cells in Figure 1 represent unidirectional composites with 60% fiber volume fraction.

Basic discretization scheme of the HFGMC model is shown in Figure 2. The two-dimensional model for unidirectional fiber-reinforced materials is based on the assumption that fibers extend in the x_1 - direction and are arranged in a doubly periodic array in the x_2 and x_3 directions. The coordinate system used for the HFGMC model corresponds to the material coordinate system of the composite ply, as x_1 is aligned with the fiber direction, x_2 lies in the ply plane and x_3 is perpendicular to the ply plane.

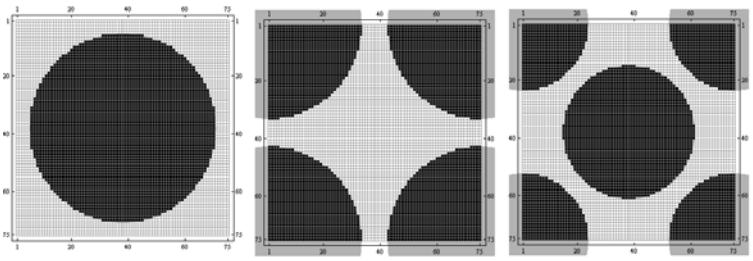

Figure 1. Composite material unit cell types analyzed in this work (75 x 75 subcells, V_f = 60%).

The input variables for the HFGMC model are the current state of macroscopic strain, number of subcells (N_β and N_γ), as well as parameters which define properties of the composite material – fiber and matrix mechanical properties and fiber volume fraction (V_f). Each subcell is selected to be a fiber or matrix constituent, based on the fiber volume fraction, number of fibers within the unit cell and position of fiber centers. At the current phase of the research dimensions of all subcells are equal and N_β is equal to N_γ, since this generalization simplifies programming of the sparse implementation of the theory. Generally, the HFGMC theory places no restrictions on the shapes of the unit cell and refinement (N_β and N_γ).

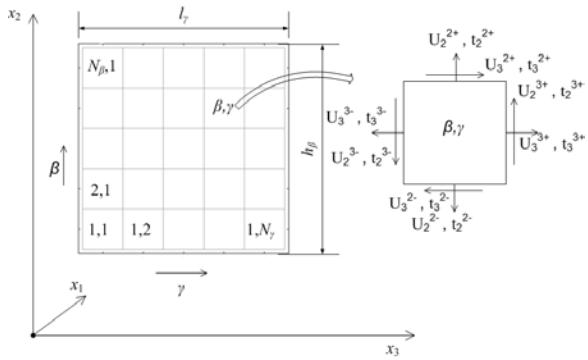

Figure 2. Discretization sheme of the HFGMC model.

As the theory of the reconstructed HFGMC micromechanical model is very complex, this work features only some basic equations which are necessary to get an insight into the procedure. More detailed explanation and discussion on the original and reconstructed HFGMC models can be found in [1,2,3,10].

The aim of the micromechanical analysis is to determine the fourth order strain concentration tensor $\mathbf{A}^{(\beta,\gamma)}$, which relates the strain tensor of each subcell $\overline{\boldsymbol{\varepsilon}}^{(\beta,\gamma)}$ to the macroscopic strain field $\overline{\boldsymbol{\varepsilon}}$, after Equation 1

$$\overline{\boldsymbol{\varepsilon}}^{(\beta,\gamma)} = \mathbf{A}^{(\beta,\gamma)}\overline{\boldsymbol{\varepsilon}}\,. \tag{1}$$

The displacement field within the unit cell is approximated using the same Legendre-type polynomial expansion of the original HFGMC, after [10].

$$\begin{aligned} u_i^{(\beta,\gamma)} &= \overline{\varepsilon}_{ij}x_j + W_{i(00)}^{(\beta,\gamma)} + \overline{y}_2^{(\beta)}W_{i(10)}^{(\beta,\gamma)} + y_3^{(\gamma)}W_{i(01)}^{(\beta,\gamma)} \\ &+ \frac{1}{2}\left(3y_2^{(\beta)2} - \frac{h_\beta^2}{4}\right)W_{i(20)}^{(\beta,\gamma)} + \frac{1}{2}\left(3y_3^{(\gamma)2} - \frac{l_\gamma^2}{4}\right)W_{i(02)}^{(\beta,\gamma)}, \qquad i,j = 1,2,3. \end{aligned} \tag{2}$$

The first term on the right side of Equation 2 represents the contribution of the homogenized (averaged) strain, while the rest represents the fluctuating displacement field ($u_i'^{(\beta,\gamma)}$). The W variables in Equation 2 are microvariables, which define the fluctuating displacement field within each subcell. These microvariables have to be determined in order to calculate the strain field within the unit cell. The solution of the micromechanical model begins by defining subcell local stiffness matrices, which are assembled into the global system by application of traction and continuity conditions at subcell interfaces and periodicity equations at unit cell boundaries, as explained in [1,2]. The global system of equations can be decoupled into axial and transverse sets of equations, after [3]. The components of strain tensor in Equations 3 and 4 are referred to homogenized or equivalent deformations of the complete unit cell

$$\begin{bmatrix} \mathbf{L}_{11} & \Delta\mathbf{c}\mathbf{L}_{12} \\ \mathbf{L}_{21} & \Delta\mathbf{c}_{22} \end{bmatrix} \begin{Bmatrix} \mathbf{0}\,\bar{\mathbf{u}}_1'^{2} \\ \bar{\mathbf{u}}_1'^{3} \end{Bmatrix} = \begin{bmatrix} {}_{11} & \\ \mathbf{0} & {}_{22} \end{bmatrix} \begin{Bmatrix} \bar{\varepsilon}_{12} \\ \bar{\varepsilon}_{13} \end{Bmatrix}, \tag{3}$$

$$\begin{bmatrix} \mathbf{K}_{11} & \mathbf{0} & \mathbf{K}_{13} & \mathbf{K}_{14} \\ \mathbf{0} & \mathbf{K}_{22} & \mathbf{K}_{23} & \mathbf{K}_{24} \\ \mathbf{K}_{31} & \mathbf{K}_{32} & \mathbf{K}_{33} & \mathbf{0} \\ \mathbf{K}_{41} & \mathbf{K}_{42} & \mathbf{0} & \mathbf{K}_{44} \end{bmatrix} \begin{Bmatrix} \bar{\mathbf{u}}_2'^{2} \\ \bar{\mathbf{u}}_3'^{2} \\ \bar{\mathbf{u}}_2'^{3} \\ \bar{\mathbf{u}}_3'^{3} \end{Bmatrix} = \begin{bmatrix} \Delta\mathbf{C}_{11} & \Delta\mathbf{C}_{12} & \Delta\mathbf{C}_{13} & \mathbf{0} \\ \mathbf{0} & \Delta\mathbf{C}\,\mathbf{0} & \mathbf{0} & {}_{24} \\ \mathbf{0} & \Delta\mathbf{C}\,\mathbf{0} & \mathbf{0} & {}_{34} \\ \Delta\mathbf{C}_{41} & \Delta\mathbf{C}_{42} & \Delta\mathbf{C}_{43} & \mathbf{0} \end{bmatrix} \begin{Bmatrix} \bar{\varepsilon}_{11} \\ \bar{\varepsilon}_{22} \\ \bar{\varepsilon}_{33} \\ \bar{\varepsilon}_{23} \end{Bmatrix}. \tag{4}$$

The size of the global axial system of equations (Equation 3) is $2N_\beta N_\gamma \times 2N_\beta N_\gamma$, while the transverse system of equations (Equation 4) consists of $4N_\beta N_\gamma \times 4N_\beta N_\gamma$ elements. Global **L** and **K** matrices are assembled from subcell local stiffness matrices as explained in [2,3]. The submatrices $\Delta\mathbf{c}$ (in Equation 3) and $\Delta\mathbf{C}$ (in Equation 4) contain differences in elastic stiffness elements $C_{ij}^{(\beta,\gamma)}$ between adjacent subcells. The constitutive behavior of matrix subcells is assumed to be isotropic, while fiber subcells are orthotropic. The mechanical properties of the T300 carbon fiber and 5208 epoxy matrix are summarized in Table 1 [12 - 14]. The equivalent properties of a CFRP composite with 70% fiber volume fraction calculated by the HFGMC are also listed in Table 1.

The displacement vectors in Equations 3 and 4 are comprised of subcell fluctuating interface displacements. The solution of the global system of equations enables calculation of the displacement field within the unit cell. Once the solution of the unit cell displacement field has been obtained, microvariables W can be computed allowing calculation of strain tensor components using [3]

$$\begin{aligned}
\varepsilon_{11}^{(\beta,\gamma)} &= \bar{\varepsilon}_{11}, \\
\varepsilon_{22}^{(\beta,\gamma)} &= \bar{\varepsilon}_{22} + W_{2(10)}^{(\beta,\gamma)} + 3\bar{y}_2^{(\beta)} W_{2(20)}^{(\beta,\gamma)}, \\
\varepsilon_{33}^{(\beta,\gamma)} &= \bar{\varepsilon}_{33} + W_{3(01)}^{(\beta,\gamma)} + 3\bar{y}_2^{(\beta)} W_{3(02)}^{(\beta,\gamma)}, \\
\varepsilon_{12}^{(\beta,\gamma)} &= \bar{\varepsilon}_{12} + \frac{1}{2}\left[W_{1(10)}^{(\beta,\gamma)} + 3\bar{y}_2^{(\beta)} W_{1(20)}^{(\beta,\gamma)} \right], \\
\varepsilon_{13}^{(\beta,\gamma)} &= \bar{\varepsilon}_{13} + \frac{1}{2}\left[W_{1(01)}^{(\beta,\gamma)} + 3\bar{y}_3^{(\gamma)} W_{1(02)}^{(\beta,\gamma)} \right], \\
\varepsilon_{23}^{(\beta,\gamma)} &= \bar{\varepsilon}_{23} + \frac{1}{2}\left[W_{2(01)}^{(\beta,\gamma)} + 3\bar{y}_3^{(\gamma)} W_{2(02)}^{(\beta,\gamma)} + W_{3(10)}^{(\beta,\gamma)} + 3\bar{y}_2^{(\beta)} W_{3(20)}^{(\beta,\gamma)} \right].
\end{aligned} \tag{5}$$

The strain concentration tensor is obtained using a numerical procedure explained in [2]. Finally, the average subcell stress field $\overline{\boldsymbol{\sigma}}^{(\beta,\gamma)}$ is computed based on subcell constitutive model and subcell strain tensors $\overline{\boldsymbol{\varepsilon}}^{(\beta,\gamma)}$

$$\overline{\boldsymbol{\sigma}}^{(\beta,\gamma)} = \mathbf{C}^{(\beta,\gamma)}\overline{\boldsymbol{\varepsilon}}^{(\beta,\gamma)}. \tag{6}$$

The unit cell macroscopic stresses can be obtained by averaging the microscopic stress over the unit cell using equation

$$\overline{\boldsymbol{\sigma}} = \frac{1}{hl}\sum_{\gamma=1}^{N_\gamma}\sum_{\beta=1}^{N_\beta} h_\beta l_\gamma \mathbf{C}^{(\beta,\gamma)}\mathbf{A}^{(\beta,\gamma)}\overline{\boldsymbol{\varepsilon}}, \tag{7}$$

while the equivalent elasticity tensor is calculated using Equation 10

$$\mathbf{C}^* = \frac{1}{hl}\sum_{\gamma=1}^{N_\gamma}\sum_{\beta=1}^{N_\beta} h_\beta l_\gamma \mathbf{C}^{(\beta,\gamma)}\mathbf{A}^{(\beta,\gamma)}. \tag{8}$$

T 300 fiber	5208 epoxy matrix	T300/5208 composite
$E_1 = 258.57$ GPa	$E = 3.4$ GPa	$E_1 = 182.61$ GPa
$E_2 = E_3 = 18.69$ GPa	$v = 0.35$	$E_2 = 11.29$ GPa
$v_{12} = 0.2$	$T_m = 50$ MPa	$G_{12} = 6.10$ GPa
$v_{23} = 0.4$	$C_m = 100$ MPa	$v_{12} = 0.237$
$G_{12} = 19.68$ GPa	$T = 25$ MPa	$v_{23} = 0.391$

Table 1. Fiber and matrix properties and HFGMC predicted composite properties.

2.2 Micromechanical failure criteria

Micromechanical failure criteria determine failure initiation within the unit cell at the micro constituent level (fiber or matrix). The attention in this work has been given to failure criteria associated with matrix failure. Based on a literature survey on micromechanical composite failure criteria for unidirectional composites, two criteria have been selected for implementation:

1) 3-D Tsai –Hill criterion, after [7]

$$\frac{\left(\overline{\sigma}_{11}^{(\beta,\gamma)}\right)^2 + \left(\overline{\sigma}_{22}^{(\beta,\gamma)}\right)^2 + \left(\overline{\sigma}_{33}^{(\beta,\gamma)}\right)^2}{Y^2} + \frac{\overline{\sigma}_{11}^{(\beta,\gamma)}\overline{\sigma}_{22}^{(\beta,\gamma)} + \overline{\sigma}_{11}^{(\beta,\gamma)}\overline{\sigma}_{33}^{(\beta,\gamma)} + \overline{\sigma}_{22}^{(\beta,\gamma)}\overline{\sigma}_{33}^{(\beta,\gamma)}}{Y^2} + \frac{\left(\overline{\sigma}_{12}^{(\beta,\gamma)}\right)^2 + \left(\overline{\sigma}_{13}^{(\beta,\gamma)}\right)^2 + \left(\overline{\sigma}_{23}^{(\beta,\gamma)}\right)^2}{T^2} = d_m^2 . \tag{9}$$

The 3D Tsai-Hill criterion has been used in [7] to predict transverse cracking in matrix constituent subcells. The Y variables in Equation 9 are matrix strengths (tensile - T_m or compressive - C_m), while T is the matrix shear strength. The necessary properties for calculation of failure criteria for the 5208 epoxy matrix are listed in Table 1.

2) Micromechanics of Failure criterion for matrix failure (MMF), after [12]

$$\frac{\bar{\sigma}_{VM}^{(\beta,\gamma)2}}{T_m C_m} + \left(\frac{1}{T_m} - \frac{1}{C_m}\right) I_1^{(\beta,\gamma)} = 1, \tag{10}$$

where $\bar{\sigma}_{VM}^{(\beta,\gamma)}$ is the equivalent subcell stress, while $I_1^{(\beta,\gamma)}$ is the first invariant of the stress tensor of the subcell. Variables T_m and C_m in Equation 10 are matrix tensile and compressive strengths (such as listed in Table 1).

3 Multiscale analysis

The multiscale procedure has been tested on a simple composite plate. The plate consists of four unidirectional CFRP plies with the layup [90/45/45/90]. The thickness of each ply is 0.125 mm, while the dimensions of the plate are 0.3 x 0.2 m. The orientation of the composite plies is measured with regard to the longer plate dimension (*x*-axis in Figure 3). The constitutive behavior of the homogenized CFRP material has been predicted by HFGMC for a composite with 70% fiber volume fraction. The equivalent properties have been calculated using a 100 x 100 unit cell with a single fiber at the unit cell centre and are summarized in Table 1. The leading idea behind this evaluation is to select a useful ply-level criteria which will trigger the HFGMC model and damage evolution procedure on the unit cell micromechanical model. Therefore, micromechanically calculated failure criteria of the matrix have been compared to the most commonly used ply level criteria (Tsai-Wu, Tsai Hill, Hashin and Puck).

The finite element model (shown in Figure 3) consists of 150 S4R finite elements and 176 nodes, resulting in 1056 degrees of freedom of the numerical model. In order to investigate the effect of unit cell refinement, three refinement levels have been selected in the two scale approach – 20 x 20 , 50 x 50 and 75 x 75. The composite plate has been loaded with a tensile force of 5500 N (500 N per node).

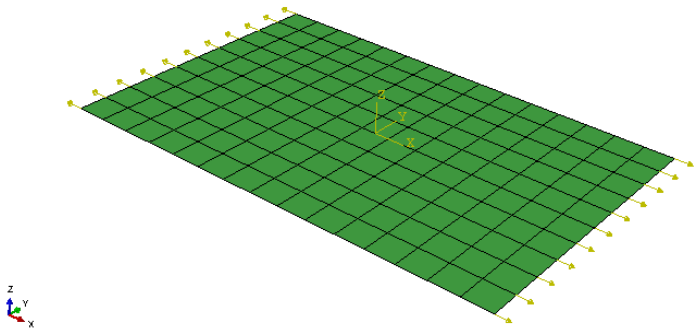

Figure 3. Numerical model used for multiscale implementation.

3.1 Implementation of HFGMC in Abaqus

Abaqus user material subroutine VUMAT has been used to implement the micromechanical model into the finite element analysis. The work described in this paper is in the initial phase of implementation of the multiscale computational model, and therefore material properties have not been degraded due to damage effects. The HFGMC model is programmed as a subroutine which is called from within Abaqus/Explicit user material subroutine VUMAT. Input parameters in the subroutine are the current macroscopic strain state and parameters which define the unit cell (N_β, N_γ, number and position of fiber etc.). The systems of Equations 3 and 4 result in highly sparsed matrices. In order to enable modeling of finer unit cells (and consequently solving larger systems of equations), a sparse implementation has been introduced to obtain solution of the HFGMC model. In addition to finer unit cell

discretization, sparse implementation of HFGMC resulted in significant improvement of computational time. The output from the HFGMC model are composite equivalent properties and maximal values of subcell micromechanical failure criteria. These values are stored in the VUMAT subroutine as state dependent variables (SDVs).

4 Results

In the analyzed load case, fiber failure is not likely to occur (maximal value of damage initiation criteria associated with fiber failure is 0.305 - Hashin's fiber tensile criterion), and therefore the attention has been redirected to matrix failure. The results of the applied micromechanical matrix failure criteria in the two-scale analysis have been summarized in Table 2. The values listed in Table 2 refer to the maximal results of state dependent variables associated with micromechanical matrix failure criteria of the finite element model.

Unit cell type:	Criterion:	20x20		50x50		75x75	
		90°	45°	90°	45°	90°	45°
	3D TH	2.249	1.931	4.173	3.406	3.622	2.980
	MMF	3.500	3.130	8.798	6.841	6.963	5.571
	3D TH	2.243	1.926	4.171	3.405	3.201	2.660
	MMF	3.488	3.122	8.791	6.837	5.754	4.747
	3D TH	0.951	0.921	0.961	0.929	1.042	1.065
	MMF	1.197	1.241	1.219	1.264	1.414	1.460

Table 2. Maximal values of micromechanical matrix failure criteria in the FE model.

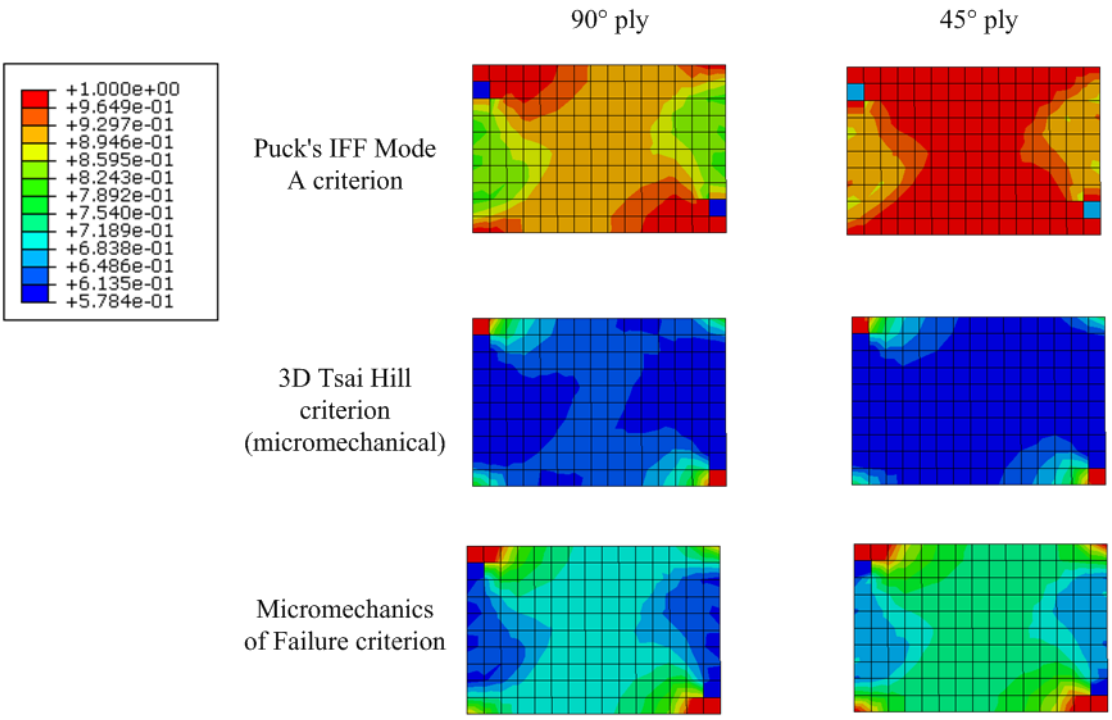

Figure 4. Comparison of failure initiation criteria - Puck's Mode A IFF criterion and micromechanical matrix failure criteria calculated on a 5-fibre unit cell with 75 x75 subcells.

As indicated in Table 2, the results show significant discrepancies and dependence on both examined parameters - unit cell type and refinement of the HFGMC micromechanical model. Micromechanical failure criteria calculated using the unit cell with a central fiber and the morphology with fibers on the unit cell corners predict failure initiation at lower load states compared to the applied ply level criteria. As a consequence, the micromechanical failure

initiation criteria reach higher values (left-hand sides of Equations 9 and 10) in the finite element model and predict failure initiation over the entire FE model. In contrast, the unit cell with 5 fibers predicts lower values of matrix failure criteria compared to ply-level criteria, as shown in Figure 4. Figure 4 shows a comparison of the macromechanically calculated Puck's interfiber (IFF) Mode A criterion and both applied micromechanical failure theories for the 5 fiber unit cell type discretized with 75 x 75 subcells. The 3D Tsai Hill and Micromechanics of Failure criteria predict failure initiation in a very similar portion of the finite element model, although at a much smaller part compared to the ply level Puck's criteria, especially for the 45° plies. The contours of the micromechanically predicted failure criteria using the unit cells with a central fiber and the unit cells with fibers on the corners agree well with the contours shown in Figure 4 (for the unit cell with 5 fibers), while the values are much higher (as presented in Table 2).

The material points of the finite element model with maximal values of the micromechanical matrix failure criteria are located in the corners of the composite plate, as shown in Figure 4. The distribution of the micromechanical matrix failure criteria within the unit cell has been evaluated for a material point of the FE model for which all applied ply level failure criteria (Tsai-Wu, Tsai-Hill, Hashin's matrix tensile and Puck's IFF Mode A criteria) reach, in the given load case, the critical value, thereby indicating initiation of damage processes. The distribution of matrix failure criteria within the three investigated unit cells, along with the effect of unit cell refinement is shown in Figures 5 and 6.

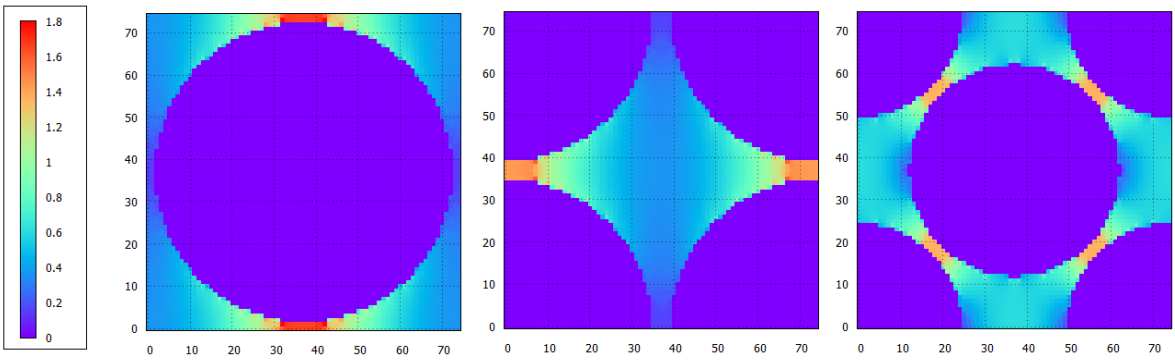

Figure 5. Effect of unit cell type on 3D Tsai Hill criterion (HFGMC model with 75 x 75 subcells).

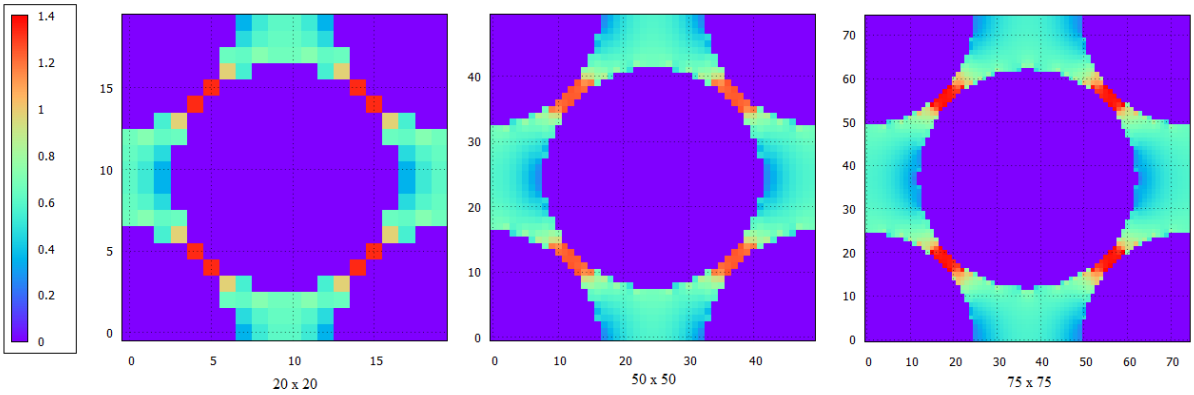

Figure 6. Effect of unit cell refinement on distribution of Micromechanics of Failure matrix damage initiation criterion.

The effect of unit cell type on the distribution of the 3-D Tsai-Hill criterion is shown in Figure 5. The unit cell with a single fiber reaches the highest value of the criterion (1.779), followed

by the unit cell with fibers on the unit cell corners (1.588). These two unit cells show similar distribution of the matrix damage criteria, which is reasonable, since these two discretization schemes present the same composite system. The unit cell with fibers on the corners and in the centre of the unit cell shows the lowest value of the evaluated matrix failure criterion (1.386). The effect of unit cell refinement on the results is shown in Figure 6 on the example of the Micromechanics of Failure criterion and the unit cell with fibers on the corners and in the centre of the unit cell. The highest values of failure criteria are reached at the subcells in the areas of the unit cell where the distance between separate fibers is the least. The maximal values (1.398 for the 75 x 75 unit cell) are located in matrix subcells which directly surround the fiber.

5 Conclusion

This work presents results of the initial phase of implementation of the HFGMC model in an explicit finite element code. The HFGMC model has been used to calculate equivalent composite properties and micromechanical matrix failure criteria. In the ongoing research, the HFGMC model is employed to predict equivalent composite properties after damage initiation caused by impact loading, blast loads and similar high velocity / high strain phenomena.

The results in this work indicate significant dependence of the micromechanical matrix failure criteria on the unit cell type and refinement. The micromechanical criteria on the HFGMC model tend to be more restrictive when compared to the most commonly used ply-based failure criteria as they reach critical values at lower loading states. An exception is the unit cell with fibers on unit cell corners and at the centre, which for a given loading state predicts lower values of matrix failure criteria. The effect of unit cell refinement on the values of failure criteria is not fully understood, but finer levels of the HFGMC mesh result in improved distribution of the micromechanical stresses thereby improving the distribution of failure criteria. A HFGMC mesh with smaller subcells will also allow more accurate modeling of damage processes in the continuation of present work.

In order to develop the micromechanical failure prediction, further research will have to be performed. Ply level criteria indicate failure of the complete ply, whereas micromechanical criteria indicate failure at a much smaller level. Consequently, failure at the micro-level doesn't necessarily indicate failure of the complete ply. Therefore, a reasonable correlation between failure prediction on the micro-level and ply-level based failure criteria or experimental results is expected after inclusion of damage processes in the HFGMC model. Furthermore, the influence of the interphase at the matrix/fiber boundaries will have to be included in the micromechanical analysis, since effects at the interphase play a significant role in damage mechanisms of composite materials [15]. As illustrated by the failure criteria in Figures 5 and 6, maximal values of failure criteria are predicted in matrix subcells which surround the fibers, additionally indicating the importance of correct modeling of this area of the unit cell. Despite all problems encountered during the current work, the HFGMC presents a highly promising model for further development.

References

[1] Bansal Y., Pindera M.J. Efficient Reformulation of the Thermoelastic Higher-Order Theory for FGMs. *NASA/CR–2002–211909*. (2002).

[2] Bansal Y., Pindera M.J. A Second Look at the Higher-Order Theory for Periodic Multiphase Materials. *Journal of Applied Mechanics*, **72**, pp. 177-195 (2005).

[3] Bansal Y., Pindera M.J. Finite-Volume Direct Averaging Micromechanics of Heterogeneous Materials with Elastic-Plastic Phases. *International Journal of Plasticity*, **22**, pp. 775-825 (2006).
[4] Aboudi J. Closed Form Constitutive Equations for Metal Matrix Composites. *International Journal of Engineering Science*, **25(9)**, pp. 1229-1240 (1987).
[5] Paley M., Aboudi J. Micromechanical Analysis of Composites by the Generalized Cells Model. *Mechanics of Materials*, **14**, pp. 127-139 (1992).
[6] Tang Z., Zhang B. Prediction of Biaxial Failure Envelopes for Composite Laminates Based on Generalized Method of Cells. *Composites: Part B*, **43**, pp. 914-925 (2012).
[7] Pineda M.J., Waas A.M., Bednarcyk B.A. *Multiscale Model for Progressive Damage and Failure of Laminated Composites Using an Explicit Finite Element Method* in "Proceedings of the *50th AIAA/ASME/ASCE/AHS/ASC Structures, Structural Dynamics, and Materials Conference*, Palm Springs, California, USA, (2009).
[8] Arnold S.M., Bednarcyk B., Aboudi J. Comparison of the Computational Efficiency of the Original Versus Reformulated High-Fidelity Generalized Method of Cells. *NASA/TM – 2004-213438*, (2004).
[9] Bednarcyk B.A., Arnold S.M., Aboudi J., Pindera M.J. Local Field Effects in Titanium Matrix Composites Subject to Fiber-Matrix Debonding. *International Journal of Plasticity*, **20**, pp. 1707-1737 (2004).
[10] Aboudi J., Pindera M.J., Arnold S.M. Higher-Order Theory for Periodic Multiphase Materials with Inelastic Phases. *International Journal of Plasticity*, **19**, pp. 805-847 (2003).
[11] Sun X.S., Tan V.B.C., Tay T.E. Micromechanics-Based Progressive Failure Analysis of Fibre-Reinforced Composites with Non-Iterative Element-Failure Method. *Computers and Structures*, **89**, pp. 1103-1116 (2011).
[12] Springer G.S., Kollar L.P. *Mechanics of Composite Structures*. Cambridge University Press, Cambridge (2003).
[13] Tsai S.W. *Theory of Composites Design*. Think Composites, Dayton (1992).
[14] Ehrenstein G.W. *Faserverbund-Kunststoffe*. Carl Hanser Verlag München Wien, Munich (2006).
[15] Matzenmiller A., Gerlach S. Parameter Identification of Elastic Interphase Properties in Fiber Composites. *Composites: Part B*, **37**, pp. 117-126 (2006).